Angular and high-frequency analysis of electron interference structures in ~60 MeV/u $Kr^{34+}+H_2$ collisions

J. A. Tanis,[1] J.-Y. Chesnel,[2] B. Sulik,[3] B. Skogvall,[4] P. Sobocinski,[4] A. Cassimi,[2] J.-P. Grandin,[2] L. Adoui,[2] D. Hennecart,[2] and N. Stolterfoht[4]

[1]*Department of Physics, Western Michigan University, Kalamazoo, Michigan 49008, USA*
[2]*CIRIL Unité Mixte CEA-CNRS-EnsiCaen-Université de Caen, F-14050, Caen Cedex 4, France*
[3]*Institute for Nuclear Research (ATOMKI), H-4001, Debrecen, Hungary*
[4]*Hahn-Meitner-Institut Berlin GmbH, Glienickerstrasse 100, D-14109 Berlin, Germany*

(Received 29 January 2006; published 2 August 2006)

Detailed analyses of previous measurements, combined with additional measurements reported here, have been made of electron interference structures observed in 60 MeV/u $Kr^{34+}+H_2$ collisions. Results are used to characterize the angular dependence of the primary interference structures over a wide range of electron ejection angles, particularly backward angles, and, additionally, to search for high-frequency structures as reported recently for 1–5 MeV/u $H^+ + H_2$ collisions [Hossain *et al.*, Phys. Rev. A **72**, 010701(R) (2005)]. The data for backward ejection angles, in combination with earlier data, permit a detailed comparison with theory over the range 30°–150°, showing that none of the existing theories predict accurately the observed oscillation frequencies for backward angles. Electron spectra for 90° and 150° taken in small energy steps and with improved statistics compared to earlier measurements were examined by means of a Fourier analysis but no evidence of the high-frequency structures reported for $H^+ + H_2$ collisions was found.

DOI: 10.1103/PhysRevA.74.022707 PACS number(s): 34.50.Fa, 32.80.Fb

I. INTRODUCTION

The observation [1–4] of oscillatory structures in the ejected electron energy spectra of H_2 confirmed the long-standing prediction [5] of Young-type interferences resulting from the coherent emission of electrons from identical atomic centers. Subsequent measurements showed evidence for secondary oscillations, superimposed on the main interference structures, that were attributed to additional scattering within the molecule [6]. While the primary interference structures depend strongly on the ejected electron observation angle [2,7], and to a lesser extent on the collision velocity [7], the secondary oscillations do not [6,7]. (In earlier publications the terms "first-order" and "second-order" were commonly used, but here we use "primary" and "secondary" to conform with the most recent published work [7].) Comparisons of the measured angular dependence of the primary oscillation frequencies with theoretical formulations [8–10] show fair agreement for forward angles, but the theories underestimate significantly the measured frequency for the backward angle 150°.

Very recently, evidence for additional small amplitude structures with significantly higher frequency superimposed on the secondary structures was reported for 1–5 MeV $H^+ + H_2$ collisions [7,11]. Possible origins considered for these structures were (1) coherent electron emission from the transient molecule formed by the passing H^+ ion and the H_2 molecule, and (2) interference between direct electron emission and autoionization involving *continuum* doubly excited H_2 states $2l\varepsilon l'$ giving rise to so-called free-free transitions [12]. For the former case of coherent emission, it was suggested that the colliding identical projectile and target nuclei might be a factor in producing interferences from the transient molecule that is formed [7,11], an effect that was identified theoretically for low velocity 20 keV $H^+ + H$ collisions [13]. In support of the second possibility, interference between direct emission and autoionization was recently observed for *bound* doubly excited states in $e^- + D_2$ collisions [14]. However, neither of these hypotheses for the high-frequency oscillations has been verified, and indeed the very existence of the high-frequency structures is not yet fully established.

In the present work, new measurements for 60 MeV/u Kr^{34+} ions (~40 a.u.) with experimental conditions similar to those of Refs. [1,2,6] have been made at the backward electron ejection angles 120° and 150°. The new data for 150° provide a verification of earlier results [2], for which a significantly higher frequency primary interference structure was found compared to forward angles. The data for 120° give additional information at backward angles that, when combined with previous data for forward angles [2], more fully characterize the varying oscillation frequency of the primary interference structures over a wide range of electron ejection angles. These results are compared with predictions of three different theoretical formulations. Additionally, data taken in small energy steps with improved statistics compared to earlier measurements have been obtained at 90° and 150° for the purpose of providing further insight into the previously reported evidence for high-frequency structures associated with electron emission in 1–5 MeV $H^+ + H_2$ collisions [7,11]. The use of fast krypton projectiles (~60 MeV/u) provides an important test because the observation of similar high-frequency structures for these heteronuclear collisions would rule out the hypothesis of coherent emission from the transient molecule consisting of identical atomic centers. On the other hand, if no high-frequency structures are found for krypton projectiles, coherent emission from transient molecules consisting of identical atomic centers remains a possibility.

II. EXPERIMENTAL PROCEDURE

The present measurements were carried out at the Grand Accélérateur National d'Ions Lourds (GANIL) facility in Caen, France. Since the experimental setup consisting of the scattering chamber and the electron spectrometer was nearly the same as that used in the work of Refs. [1,2,6], only a brief summary is given here. A beam of 60 MeV/u Kr^{34+} ions with a current of ~ 2 μA was collimated to a size of about 2×2 mm and directed onto a H_2 target of ~ 4 mm diameter obtained from a gas jet. Electrons emitted from the target were measured with a parallel-plate electron spectrometer for energies ranging from about 2–300 eV and for angles of 90°, 120°, and 150° with respect to the incident beam direction. For 90° and 150° the spectra were taken in small energy steps to search for high-frequency structures. At the backward angles 120° and 150° it is difficult to obtain reliable data for the higher electron energies due to the significantly smaller cross sections for backscattering. For all measurements the target gas pressure was kept below $\sim 3\times 10^{-5}$ Torr, corresponding to a range where single-collision conditions prevailed. Additionally, background spectra were recorded with no target gas so that the spectra of interest could be corrected for these residual gas events. Care was also taken in the experimental setup to ensure that contaminants were not inadvertently introduced into the H_2 target gas. As a check, no measurable Auger intensity from common contaminants such as C, N, or O were observed in the spectra.

III. RESULTS AND DISCUSSION

Here the new measurements for the backward angles 120° and 150° are combined with our earlier data for forward angles [2] to analyze the varying oscillation frequency of the primary interference structures. Additionally, the small energy-step size data for 90° and 150° are subjected to Fourier analysis to determine if there is evidence for the high-frequency oscillatory structures reported for 1–5 MeV $H^+ + H_2$ collisions [7,11]. In the following, these angular dependent and high-frequency aspects are treated separately.

A. Angular dependence of interference structures

In order to examine the expected relatively small interference structures as a function of ejected electron velocity, the exponentially decreasing cross sections for the ionization of H_2 are normalized to the corresponding theoretical atomic H cross sections, as in Refs. [1,2].

$$(\sigma_{H_2})_{norm} = \frac{d^2\sigma_{H_2}}{d\Omega\, d\varepsilon} \Big/ \frac{d^2\sigma_{2H}}{d\Omega\, d\varepsilon} = \int \frac{d^3\sigma_{2H}}{d\mathbf{q}\, d\Omega\, d\varepsilon}\left[1+\frac{\sin|\mathbf{k}-\mathbf{q}|d}{|\mathbf{k}-\mathbf{q}|d}\right] \times d\mathbf{q} \Big/ \int \frac{d^3\sigma_{2H}}{d\mathbf{q}\, d\Omega\, d\varepsilon} d\mathbf{q}. \quad (1)$$

In Eq. (1), the solid angle $d\Omega$ and the energy $d\varepsilon$ refer to the outgoing electron, σ_{H_2} denotes the molecular cross section for two-center electron emission, and σ_{2H} is the cross section for incoherent (i.e., noninterfering) electron emission from the two H atoms. The sinusoidal term represents the interference caused by coherent emission from the two centers, where $|\mathbf{k}-\mathbf{q}|$ is the difference between the outgoing electron momentum $\mathbf{k}$ and the momentum transfer $\mathbf{q}$, and d is the molecular internuclear distance. This normalized cross section ratio $(\sigma_{H_2})_{norm}$, which more readily reveals interference behavior in the momentum distributions of the ejected electrons than in the actual cross sections alone, is obtained after averaging over the random orientation of the internuclear H_2 axis.

In calculating experimental and theoretical ratios from Eq. (1), the denominator (the atomic H cross sections integrated over the momentum transfer $\mathbf{q}$) is the same in both cases. However, in order to avoid structures produced by differences in the Compton profiles of H_2 and H [15,16], and unrelated to interferences, the effective atomic H cross sections σ_{2H} in the denominator of Eq. (1) must represent the noninterfering part of the molecular cross section σ_{H_2}. To properly represent these noninterfering cross sections, an effective atomic number $Z_{eff}=1.19$ was used to calculate the atomic H cross sections in Eq. (1) (see Ref. [15]). All of the theoretical cross sections in this work were obtained from the continuum-distorted-wave-eikonal-initial-state (CDW-EIS) approximation [17], using the formulation of this theory described in Ref. [9] that specifically includes the molecular nature of the H_2 cross sections in calculating the numerator of Eq. (1) [18].

In Fig. 1, the primary oscillatory interference features are displayed as a function of the electron momentum k (in atomic units) for the observation angles 120° and 150° with respect to the incident beam direction. The results for 150° substantially confirm the earlier results obtained for this angle [2], while the 120° data provide new information to more fully characterize the angular dependence at backward angles, particularly with respect to the frequency enhancement observed for 150°. To obtain the experimental ratios shown by the solid points, the measured doubly differential (in electron energy and observation angle) cross sections for electron emission from H_2 have been divided by the corresponding theoretical cross sections for ionization of atomic hydrogen [18] according to Eq. (1), and then plotted as a function of the electron momentum in a.u. Because of background limited statistics at 150°, the measured cross sections are reliable only for electron velocities up to ~ 2.5 a.u. (85 eV).

Also shown in Fig. 1 are the corresponding theoretical ratios calculated from the CDW-EIS formulation [9,17,18] according to Eq. (1). While there is qualitative agreement with the calculated ratios, the experimentally determined amplitudes are overestimated for low electron velocities, and the oscillation frequencies are underestimated in each case. Because the amplitude of the experimental ratios depends on the multiplication factor used to normalize the measured relative molecular H_2 electron cross sections to the theoretical atomic H cross sections, the actual value of the amplitude is arbitrary and, consequently, the discrepancy is not significant (see Ref. [2]). On the other hand, the frequency of the

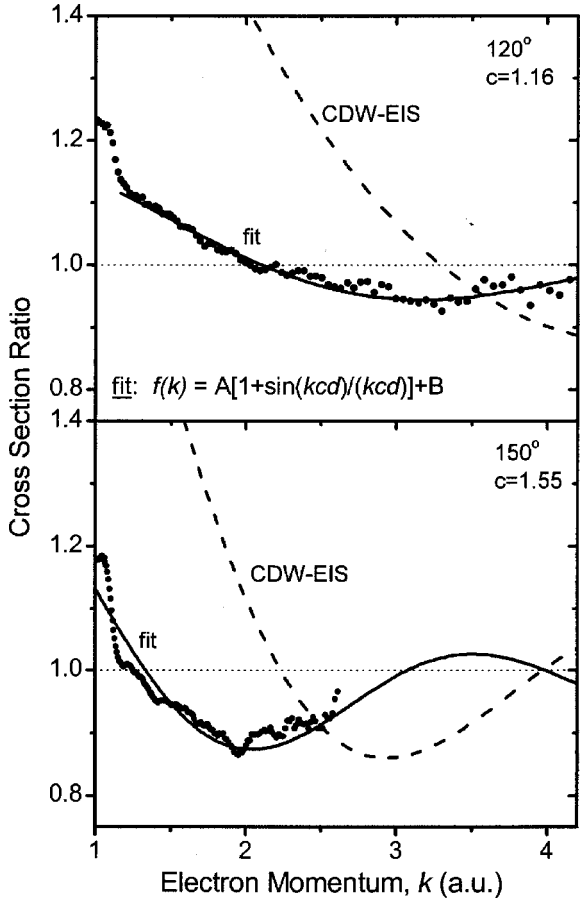

FIG. 1. Ratios of cross sections, determined according to Eq. (1), for electron emission from H_2 by 60 MeV/u Kr^{34+} impact normalized to the corresponding atomic H cross sections for the electron observation angles 120° and 150°. Solid points are the measured H_2 cross sections divided by theoretical continuum-distorted-wave-eikonal-initial-state (CDW-EIS) cross sections for atomic H [17,18]. The dashed curves are ratios of theoretical CDW-EIS cross sections for H_2 [9,18] divided by those for H. The theoretical results for atomic H were calculated using $Z_{\text{eff}}=1.19$ in the denominator of Eq. (1) to account for differences in the Compton profiles of H_2 and H (see text). The solid curves are fits to the data using Eq. (2), and the resulting values obtained for the frequency parameter c are indicated. The dotted line drawn at a cross section ratio of 1.0 indicates the limiting value of the sinusoidal function appearing in Eqs. (1) and (2).

oscillation does not depend on the normalization factor (the calculated frequencies in Ref. [2] are the same as those found here), and, hence, a meaningful comparison between experiment and theory can be made. Concerning the underestimation of the measured frequencies, similar discrepancies have been found previously for Kr^{34+} projectiles [2] and for H^+ projectiles [7,11].

In order to parametrize the changing frequency, an analytical function of the form

$$f(k) = A[1 + \sin(kcd)/(kcd)] + B \tag{2}$$

was fit to the normalized ratios of Fig. 1, a procedure that has been used previously [2,6,7,11]. In this function, A and B

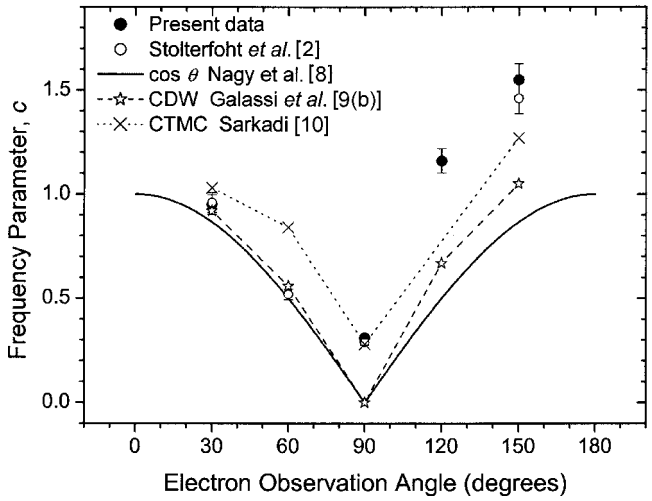

FIG. 2. Experimental and theoretical values of the primary interference frequency parameter c as a function of the electron observation angle. The solid (present data) and open (from Ref. [2]) symbols were obtained by fitting Eq. (2) to cross section ratios as shown in Fig. 1, while the theoretical values were taken from Refs [8–10] as indicated.

($A+B\approx 1$, see Ref. [2]) are constants representing the interfering and noninterfering cross section fractions, respectively, and c is an adjustable frequency parameter. This function is based on the impact-parameter formulation of Nagy *et al.* [8], where it is found that $|\mathbf{k}-\mathbf{q}|$ in Eq. (1) can be approximated by $(k\cos\theta - q_{\min})$, i.e., the electron momentum component parallel to the beam direction (θ is the electron observation angle) minus the minimum momentum $q_{\min}$ transferred in the collision. Here, $q_{\min}=\Delta E/v_p$ where ΔE is the energy transferred to the electron and v_p is the velocity of the projectile. Hence, for the high collision velocity of the present work $q_{\min}\sim 0$, and $c\sim\cos\theta$ in the model of Nagy *et al.* [8]. The results of fitting Eq. (2) to the data of Fig. 1, shown as the solid curves, are seen to represent well the measured cross section ratios.

Values of the frequency parameter c obtained from the fit function Eq. (2) for the present data, as well as the earlier data for Kr^{34+} projectiles from Ref. [2], are plotted in Fig. 2 as a function of the electron observation angle θ. Also shown are the calculated values of the frequency parameter from the formulation of Nagy *et al.* [8] (in which $c\sim\cos\theta$), the CDW-EIS calculations of Galassi and co-workers [9], and the classical-trajectory-Monte-Carlo (CTMC) calculations of Sarkadi [10]. While there is qualitative agreement of the experimentally determined values of c with the trends predicted by the calculations, and moreover the observed variations in c with electron ejection angle can be understood in terms of the above-mentioned dependence on $(k\cos\theta - q_{\min})$, there are also significant and systematic discrepancies, particularly for backward angles. The new measurements for 120° confirm the rather strong asymmetry in the oscillation frequency, by nearly a factor of 2, previously observed for 30° and 150°, while the calculations predict a nearly symmetric dependence, with the exception perhaps of the CTMC calculations of Ref. [10].

These various discrepancies suggest that the existing theories do not properly describe the angular dependence of

the oscillation frequency, particularly with respect to complementary forward and backward angles. While the exact origin of the frequency asymmetry is not known, it is noted that electron emission at backward angles involves significant backscattering [19]. Furthermore, such backscattering is required to produce the secondary interferences that have been observed to have 2–3 times higher frequencies than the primary interference structures [6,7]. Thus, there may be an interplay of the secondary interferences with the primary ones that gives rise to enhancement of the oscillation frequency [20]. However, the exact characterization of the enhanced frequencies for backward angles remains a challenge for theory.

B. Search for high-frequency structures

Here we examine the electron spectra for the existence of structures with much higher frequencies than the primary oscillations discussed above, and also significantly higher than the secondary oscillations (not considered in the present work) that have been attributed to intramolecular scattering of the primary ionization "wave" at the second atomic center [6]. These secondary oscillations, which are superimposed on the primary oscillations and expected to exhibit one full oscillation in the range of electron velocities from $\sim 1-3$ a.u. [6], are not apparent in the experimental ratios of Fig. 1 without further analysis. However, the existence of these secondary oscillations has been confirmed in $H^+ + H_2$ collisions [7,11] for both forward and backward emission angles. Since an examination of the secondary oscillations is not the intent of the present work they will not be considered further here.

Evidence for high-frequency structures, superimposed on the primary and secondary interference structures, was reported in electron spectra associated with ionization of H_2 by 1, 3, and 5 MeV H^+ ions [7,11]. By fitting the oscillations with a function similar to Eq. (2), but without the damping of the sine term, a high-frequency oscillation interval corresponding to $\Delta k \sim 0.25$ a.u. was determined [11]. As noted in the Introduction, no definitive conclusions concerning either the existence or the origin of the oscillations have been reached. More recently, anomalous oscillations with high frequencies similar to those of Refs. [7,11] were observed in the ionization spectra of 20 keV He^+ and 40 keV He^{2+} ions colliding with atomic He [21]. Again, several causes of the oscillations were considered but no conclusion could be made regarding their origin.

As mentioned above, data were taken in small energy steps for 90° and 150° to determine if there is evidence for high-frequency structures in the electron spectra for the fast 60 MeV/u $Kr^{34+} + H_2$ collisions studied here. The measured electron momentum spectra were subjected to Fourier analysis to ascertain if the transformed inverse momentum spectra contain discrete components corresponding to high oscillation frequencies. In this analysis the raw electron spectra, following background subtraction and conversion of the energy scale (in eV) to electron momentum k (in a.u.), were subjected directly to Fourier transformation, rather than using the normalized ratios. The raw spectra were used to minimize the possibility of introducing spurious oscillatory structures resulting from the normalization of the data to theoretical cross sections (spurious structures can be introduced depending on the step size of the theoretical calculations used for normalization). Additionally, the spectra were smoothed using three-point and five-point adjacent averaging and then subjected to the same Fourier analysis, giving results essentially identical to those for the raw spectra.

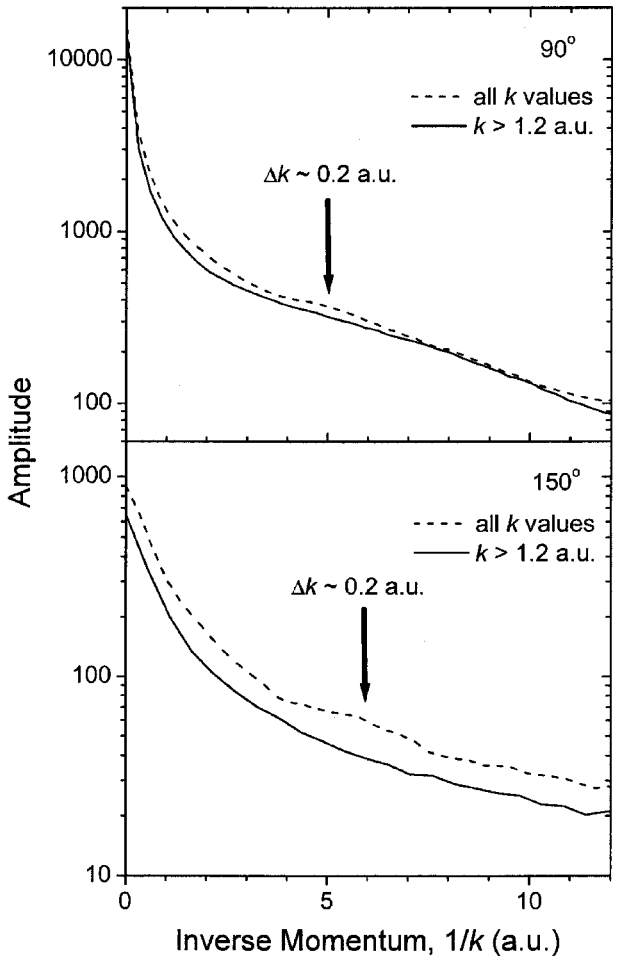

FIG. 3. Inverse spectra resulting from the Fourier analysis of measured electron momentum spectra, after residual background subtraction and conversion of the measured electron energy values (in eV) to electron momentum k (in a.u.), for the observation angles 90° and 150°. The Fourier analysis was carried out for all k values (dashed curves) and for the restricted range $k > 1.2$ a.u. (solid curves). The small maximum near $1/k = 5$ a.u, corresponding to an electron momentum oscillation interval of $\Delta k \sim 0.2$ a.u., seen in the dashed curves in each case, is attributed to the H_2^* autoionization peak that occurs near 1 a.u. (see Fig. 1).

The inverse momentum spectra resulting from Fourier transformation of the electron momentum spectra are shown in Fig. 3 for the observation angles 90° and 150°. The dashed curve in each case is the inverse spectrum that results when the measured momentum spectrum is analyzed for the entire range of measured k values, whereas the solid curve is the result when the spectrum is subjected to analysis only for $k > 1.2$ a.u. The reason for using this latter reduced range is to eliminate any effect due to the peak that occurs in the momentum spectra near $k \sim 1.0$ a.u. (see Fig. 1). This peak,

which is attributed to autoionization of doubly excited H_2^* [1,14], has a width $\Delta k \sim 0.2$ a.u. (see Fig. 1) that is coincidentally close to the width $\Delta k \sim 0.25$ a.u. expected for the high-frequency structures based on the results for $H^+ + H_2$ collisions [11].

The Fourier transformed inverse momentum spectra of Fig. 3 show strongly decreasing intensities with increasing $1/k$ (larger values of $1/k$ correspond to higher frequencies in the electron momentum spectrum). Based on a width $\Delta k \sim 0.25$ a.u. (see above), a discrete component corresponding to high-frequency structures would be expected in the inverse spectrum near $1/k \sim 4$ a.u. if such structures exist. No such component is observed in the solid curves of Fig. 3 resulting from Fourier analysis for electron velocities $k > 1.2$ a.u. Instead, these curves decrease monotonically up to values of $1/k > 10$ a.u. in each case. On the other hand, Fourier analysis for all k values (dashed curves) for both 90° and 150° shows a small and broad maximum centered near $1/k \sim 5$ a.u. corresponding to an electron momentum width $\Delta k \sim 0.2$ a.u. Thus, this maximum in the dashed curves can be attributed to the presence of the H_2^* autoionization peak that occurs near $k=1$ a.u. The observation of this maximum for the transformation over all k values is important because it provides an indication of the sensitivity of the Fourier analysis in precisely the region of interest. Moreover, the inverse spectra are dominated by an intense and strongly decreasing continuum (note the logarithmic scale of Fig. 3) near zero resulting from the large nonoscillating "background" of continuum electrons in the raw momentum spectra. Thus, an observation of discrete components corresponding to the primary and secondary oscillations, expected to occur in the range $1/k < 0.7$ a.u., is precluded in the Fourier analysis. We note that essentially identical inverse spectra (not shown) were obtained when the same analysis was applied to the three-point and five-point smoothed spectra, thus giving increased confidence in the results shown in Fig. 3.

Because there is no indication of any discrete components in the inverse spectra corresponding to $k > 1.2$ a.u. in the momentum spectra, it must be concluded that the present electron emission spectra for 60 MeV/u Kr^{34+} ions do not exhibit evidence for high-frequency oscillations. Thus, the present results appear to be quantitatively different from those reported in Refs. [7,11,21] for $H^+ + H_2$ and $He^{1,2+} + He$ collisions, respectively, in which evidence for high-frequency structures was found. Additionally, it should be pointed out that the Fourier analysis, similar to that conducted here, of $H^+ + H_2$ spectra does reveal the existence of a small intensity discrete component in the inverse spectrum near $1/k \sim 4$ a.u. as expected for the high-frequency structures [22].

The lack of evidence for high-frequency oscillations in $Kr^{34+} + H_2$ collisions seems to rule out electron emission mechanisms that permit heteronuclear collision partners to be the origin of the previously reported high-frequency oscillations for $H^+ + H_2$ and $He^{1,2+} + He$ collisions. Thus, coherent emission from the transient molecule formed by homonuclear collision partners remains a possibility.

IV. CONCLUSION

In summary, we have made a detailed analysis of interference structures associated with electron emission in 60 MeV/u $Kr^{34+} + H_2$ collisions. Comparison of the measured frequencies of the primary interference structures with three different theoretical formulations shows qualitative agreement over the range 30°–150°. However, the theories do not predict the large frequency asymmetry observed for complementary forward and backward angles, and, furthermore, the calculated frequencies for backward angles underestimate the measured frequencies by 20–50 %. These results point to an incomplete understanding of the causes for the angular variation of the interference frequencies, although some of the discrepancy may originate from an interplay between the primary and secondary interferences [20].

Additionally, small step-size energy spectra for 90° and 150° have been examined for evidence of the high-frequency structures that have been reported for $H^+ + H_2$ collisions [7,11] and for $He^{1,2+} + He$ collisions [21]. Fourier analysis was used to transform the present $Kr^{34+} + H_2$ electron momentum spectra in order to reveal components in the resulting inverse spectra corresponding to high oscillation frequencies. The transformed spectra produced no such evidence, however. Thus, to summarize, evidence for high-frequency structures has been found in the spectra for electron emission from collisions involving partners with the same atomic number ($H^+ + H_2$ and $He^{1,2+} + He$), but not for partners of different atomic number ($Kr^{34+} + H_2$). This latter result is significant because it suggests the high-frequency oscillations are dependent upon homonuclear collision partners, and, consequently, coherent emission from the transient molecule formed by such partners cannot be ruled out as a possible origin.

ACKNOWLEDGMENTS

We express our gratitude to Professor P.D. Fainstein for providing us with the CDW-EIS code that was used to carry out the theoretical calculations in this work. We also acknowledge the kind assistance of Dr. Francois Frémont in carrying out the measurements at GANIL. Financial support for this work was provided by the German-French Collaboration Program PROCOPE (Contract No. 07576UH), the Hungarian OTKA (Grant No. To46905), and the German-Hungarian S&T Collaboration (D17/99).

[1] N. Stolterfoht *et al.*, Phys. Rev. Lett. **87**, 023201 (2001).
[2] N. Stolterfoht *et al.*, Phys. Rev. A **67**, 030702(R) (2003).
[3] S. Hossain *et al.*, Nucl. Instrum. Methods Phys. Res. B **205**, 484 (2003).
[4] D. Misra, U. Kadhane, Y. P. Singh, L. C. Tribedi, P. D. Fainstein, and P. Richard, Phys. Rev. Lett. **92**, 153201 (2004).
[5] H. D. Cohen and U. Fano, Phys. Rev. **150**, 30 (1966).
[6] N. Stolterfoht, B. Sulik, B. Skogvall, J. Y. Chesnel, F. Frémont,

D. Hennecait, A. Cassimi, L. Adoui, S. Hossain, and J. A. Tanis, Phys. Rev. A **69**, 012701 (2004).
[7] S. Hossain, A. L. Landers, N. Stolterfoht, and J. A. Tanis, Phys. Rev. A **72**, 010701(R) (2005).
[8] L. Nagy, L. Kocbach, K. Póra, and J. P. Hansen, J. Phys. B **35**, L453 (2002).
[9] (a) M. E. Galassi, R. D. Rivarola, P. D. Fainstein, and N. Stolterherft, Phys. Rev. A **66**, 052705 (2002); (b) M. E. Galassi, R. D. Ravarola and P. D. Fainstein, *ibid.* **70**, 032721 (2004).
[10] L. Sarkadi, J. Phys. B **36**, 2153 (2003).
[11] S. Hossain *et al.*, Nucl. Instrum. Methods Phys. Res. B **233**, 201 (2005).
[12] For an overview of autoionizing transitions, see N. Stolterfoht, Nucl. Instrum. Methods Phys. Res. B **53**, 477 (1991).
[13] J. F. Reading, J. Fu, and M. J. Fitzpatrick, Phys. Rev. A **70**, 032718 (2004).
[14] J.-Y. Chesnel, D. Martina, P. Sobocinski, O. Kamalou, F. Frémont, J. Fernándes, and F. Martín, Phys. Rev. A **70**, 010701(R) (2004).
[15] J. A. Tanis, S. Hossain, B. Sulik, and N. Stolterfoht, Phys. Rev. Lett. **95**, 079301 (2005).
[16] D. Misra, U. Kadhane, Y. P. Singh, L. C. Tribedi, P. D. Fainstein, and P. Richard, Phys. Rev. Lett. **95**, 079302 (2005).
[17] L. Gulyás, P. D. Fainstein, and A. Salin, J. Phys. B **28**, 245 (1995).
[18] The computer code used for calculations of both the molecular and atomic hydrogen cross sections was provided by P.D. Fainstein.
[19] N. Stolterfoht, R. D. DuBois, and R. D. Rivarola, *Electron Emission in Heavy Ion-Atom Collisions* (Springer, Heidelberg, 1997).
[20] N. Stolterfoht, Invited Lectures, XXIV International Conference on Photonic, Electronic, and Atomic Collisions (World Scientific Publishing, Singapore, in press).
[21] F. Frémont, A. Hajaji, A. Naja, C. Leclercq, J. Soret, J. A. Tanis, B. Sulik, and J. Y. Chesnel, Phys. Rev. A **72**, 050704(R) (2005).
[22] J. A. Tanis *et al.*, XXIV International Conference on Photonic, Electronic, and Atomic Collisions, Rosario, Argentina, 2005, Conference Program, Abstracts, edited by F. D. Colavecchia *et al.* (unpublished).